

## Calibration and validation of a non-point source pollution model

S. Grunwald<sup>a,\*</sup>, L.D. Norton<sup>b</sup>

<sup>a</sup>*Post-Doctoral Research Associate, Department of Soil Science, University of Wisconsin-Madison,  
1525 Observatory Drive, Madison, WI 53706, USA*

<sup>b</sup>*Location Coordinator, Research Leader and Director of the National Soil Erosion Research Laboratory,  
USDA — Agricultural Research Service, 1196 Soil Building, West Lafayette, IN 47907-1196, USA*

Accepted 24 August 1999

---

### Abstract

Surface runoff and sediment transport influence soil quality and the quality of receiving waters. Simulation models are useful tools to describe drainage behavior and sediment yield to develop management strategies for agricultural waters. The objective of this study was to investigate the performance of the Agricultural Non-Point Source Pollution Model (AGNPS) and modified versions comparing measured and predicted surface runoff and sediment yield at the drainage outlet. The study was carried out using 52 rainfall-runoff events from two small watersheds in Bavaria, 22 for calibration and 30 for validation. Evaluation of model outputs was based on graphical displays contrasting measured and predicted values for each rainfall-runoff event, and standard statistics such as coefficient of efficiency. A comparison between three different surface runoff methods  $Q_1$  (uncalibrated curve number (CN) method),  $Q_2$  (calibrated CN method), and  $Q_3$  (Lutz method) showed that the uncalibrated CN method underestimated measured surface runoff considerable, while the Lutz method outperformed the calibrated CN method and was better than the uncalibrated CN method. The modifications made to sediment yield calculations encompassed: (i) replacement of the Universal Soil Loss Equation  $LS$  factor algorithm by one based on stream power theory (variant  $S_2$ ), and (ii) linkage of channel erosion by individual categories of particle-size to runoff velocity (variant  $S_3$ ). The sediment yield predictions by  $S_2$  and  $S_3$  outperformed the predictions of  $S_1$  (USLE). Calculations based on  $S_3$  gave the best agreement when compared to measured sediment yield values at the drainage outlet. © 2000 Elsevier Science B.V. All rights reserved.

*Keywords:* AGNPS; Non-point source pollution; Rainfall-runoff modeling; Surface runoff; Sediment yield

---

\* Corresponding author. Tel.: +1-608-265-3331; fax: +1-608-265-2595.  
E-mail address: sgrunwald@facstaff.wisc.edu (S. Grunwald)

## 1. Introduction

An understanding of hydrological processes and sediment transport is of dual concern for the management of agricultural waters. First, surface runoff, infiltration and erosion influence soil quality and degradation. Second, these transport processes control water quality and sediment deposition of receiving waters. The event-based Agricultural Non-Point Source Pollution Model (AGNPS) (Young et al., 1987, 1994) was designed to predict runoff volume, peak flow rate, sediment and nutrient yield in medium to large-sized watersheds. The philosophy in developing AGNPS was to balance model complexity and model parameterization. A major objective was to describe major transport processes related to non-point source pollution within a landscape while using empirical and quasi-physically based algorithms. Basic model components include hydrology, sediment and nutrient transport.

Applications of the AGNPS water quality model are diverse. Feezor et al. (1989), Panuska et al. (1991), Vieux and Needhan (1993), and Grunwald (1997) investigated the effects of grid size selection through a sensitivity analysis of input. The study areas were discretized using different grid sizes, and the effect on hydrology, sediment, and nutrient components were analyzed. Model grid size was found to be the most important factor affecting sediment yield calculations. Fisher et al. (1997) analyzed the sensitivity of two distributed non-point source pollution models (AGNPS and ANSWERS) to the spatial arrangement of the landscape. This was a theoretical study, in which the input spatial data were subjected to various degrees of spatially random mixing, such that the organized landscape became disorganized. The output values of the AGNPS model exhibited little or no sensitivity to the spatial distribution of most input data. Only infiltration-related inputs produced variations in sediment and nutrient yield output. Sensitivity analyses are intended to be theoretical in nature to study model behavior.

Hession et al. (1989) linked the AGNPS model with the geographic information system (GIS) ARC/INFO and simulated effects of several best management practices assuming average input values. Linkage of the AGNPS model to a GIS was also presented by Needhan and Vieux (1989), Olivieri et al. (1991), and Tim and Jolly (1994). In those studies the emphasis was on data handling and automation of the modeling process, rather than model validation.

Use of the AGNPS model in decision support systems is widespread. Young et al. (1989) presented a study where several management practices were compared using the AGNPS model. Prato and Shi (1990) used the AGNPS model to calculate the reduction potential for erosion using several conservation practices. Tim et al. (1992) and Rode et al. (1995) used AGNPS to simulate several scenarios to compare land use and tillage practices and their impact on non-point source pollution. Grunwald et al. (1997) compared several conservation management practices that were being subsidized by a program supported by the European Union (MEKA-Program).

Validation of the AGNPS model using measured data is scarce. Panuska et al. (1991) used five rainfall-runoff events for the validation of the AGNPS model. They concluded that sediment yield calculations were highly dependent on the quality of the peak flow calculations of the model. The predicted sediment yield values ranged from a maximum underprediction of 60% to a maximum overprediction of 1.4% compared to measured

sediment yield values. Engel et al. (1993) compared the AGNPS, ANSWERS, and SWAT models using four rainfall-runoff events. AGNPS and ANSWERS showed the best results when compared to measured values. Mitchell et al. (1993) used AGNPS to compare simulated and measured values for 50 rainfall-runoff events. The deviations between the arithmetic mean of measured and simulated values were 6.3 mm for runoff volume,  $0.09 \text{ m}^3 \text{ s}^{-1}$  for peak flow rate, and 1.65 t for sediment yield. Srinivasan and Engel (1994) compared 13 measured and simulated rainfall-runoff events using AGNPS. The simulated runoff volume was underestimated for all events.

Because the AGNPS model uses many empirical and quasi-physically based algorithms, the issue of applicability in unmonitored watersheds has to be addressed. If there are no measured values for surface runoff, peak flow rate, and sediment yield no calibration and validation of the model can be carried out. In such cases the uncertainty in model simulations is high. In studies by Prato and Shi (1990), Young et al. (1989), Tim et al. (1992), and Rode et al. (1995) the AGNPS model was used in decision support studies where different land uses, tillage practices or conservation management techniques were simulated, however, no model validation was presented. Management recommendations given in those studies run the risk to proof wrong. In the studies by Panuska et al. (1991), Engel et al. (1993), and Srinivasan and Engel (1994) 5, 4, and 13 rainfall-runoff events, respectively, were used to compare predicted to measured values. Because of the small sample size it is difficult to assess model behavior. Rainfall-runoff events with high recurrence intervals may or may not be included within the total data set. No information about recurrence intervals was given in those papers.

The objective of this study was to investigate the performance of AGNPS model and modified versions comparing measured and predicted surface runoff and sediment yield at the drainage outlet of two small agricultural watersheds. The long-term goal in management of these agricultural waters is to maximize soil and water quality.

## 2. The AGNPS model

AGNPS Version 5.0 was developed by Young et al. (1987, 1994). A comprehensive description of all routines used in AGNPS can be found in the AGNPS manual (Young et al., 1987), but the AGNPS algorithms that were altered in this study are described here. AGNPS calculates surface runoff for each grid-cell separately using the SCS CN method (SCS-USDA, 1972, 1985) which can be written as

$$I_a = 0.2S, \quad (1)$$

$$S = \left( \frac{1000}{\text{CN}} - 10 \right) 25.4, \quad (2)$$

$$Q_D = \frac{(P - I_a)^2}{P + S - I_a}, \quad (3)$$

where

$Q_D$  surface runoff (mm)  
 $P$  storm precipitation (mm)

|       |                                  |
|-------|----------------------------------|
| $S$   | potential maximum retention (mm) |
| $I_a$ | initial abstraction (mm)         |
| CN    | curve number (–)                 |

The curve number is dependent on land use, soil type, and hydrologic condition. A combination of a hydrologic soil group (soil) and a land use and treatment class (cover) is a hydrologic soil-cover complex. Curve numbers are assigned to such complexes to indicate their specific runoff potential. The greater the CN, the greater the surface runoff volume. Antecedent soil moisture conditions (AMC) are considered using the total rainfall in the five-day period preceding a storm. The retention factor,  $S$ , is a constant for a particular storm because it is the maximum storage that can occur under the existing conditions. The infiltration occurring after runoff begins is controlled by the rate of infiltration at the soil surface, by the rate of transmission of water in the soil profile, or by the water-storage capacity of the profile, whichever factor is limiting. The initial abstraction ( $I_a$ ) consists mainly of interception, infiltration, antecedent soil moisture and depressional storage, all of which occur before surface runoff begins. The CN method was made to be usable with precipitation and watershed data that are ordinarily available and could be applied in unmonitored watersheds. This method estimates direct runoff, which consists of channel runoff, surface runoff, and subsurface flow in unknown proportions. The variable  $Q_D$  stands for direct runoff, which is considered equivalent to surface runoff in AGNPS (Young et al., 1987).

Surface runoff calculated in each grid-cell is routed through the watershed based on flow directions from one grid-cell to the next until it reaches the drainage outlet. There is no groundwater routine in AGNPS. The model focuses on predictions of surface water flow and sediment yield for single precipitation events only. For each grid-cell, peak flow rate is calculated using the variables drainage area, surface runoff, channel slope and size, and maximum length of path of flow into the cell considered (Smith and Williams, 1980).

$$Q_{\max} = 3.79A_{\text{EO}}^{0.7}J^{0.16}\left(\frac{Q_D}{25.4}\right)^{(0.903A_{\text{EO}}^{0.017})}\left(\frac{L^2}{A_{\text{EO}}}\right)^{-0.19}, \quad (4)$$

$$W = 2.38z^{-0.625}(1+z^2)^{0.125}\left(Q_{\max}\frac{n}{c^{0.5}}\right)^{0.375}, \quad (5)$$

$$T = \frac{zW}{2}, \quad (6)$$

$$v = \frac{\left(\frac{1.49}{n}\right)^{0.75}z^{0.25}}{0.743(2(1+z^2)^{0.5})^{0.5}c^{0.375}Q_{\max}^{0.25}}, \quad (7)$$

$$A_q = 0.5TW, \quad (8)$$

$$Q_{\text{ch}} = A_qv, \quad (9)$$

where

|                 |  |
|-----------------|--|
| $Q_{\max}$      | peak flow rate ( $\text{m}^3 \text{s}^{-1}$ )    |
| $Q_{\text{ch}}$ | channel flow rate ( $\text{m}^3 \text{s}^{-1}$ ) |

|          |  |
|----------|--|
| $A_{EO}$ | drainage area (km <sup>2</sup> )   |
| $J$      | channel slope (%)  |
| $L$      | maximum flow path (km)   |
| $W$      | width of the channel (m)   |
| $z$      | channel sideslope (%)  |
| $n$      | Manning's roughness coefficient for channel flow (m <sup>1/3</sup> s <sup>-1</sup> ) |
| $c$      | channel slope (%)  |
| $T$      | depth of channel (m)   |
| $v$      | flow velocity (m s <sup>-1</sup> )   |
| $A_q$    | cross-sectional area of the channel (m <sup>2</sup> )                                |

For each increment of the hydrograph, channel flow is calculated using channel width, channel depth, and flow velocity assuming a triangular cross-sectional area.

Soil loss is calculated by a modified Universal Soil Loss Equation (USLE) (Wischmeier and Smith, 1978), which includes the energy–intensity value and a slope shape factor.

$$A = EI K L_{USLE} S_{USLE} C P_{USLE} SSF, \quad (10)$$

where

|            |  |
|------------|--|
| $A$        | soil loss (t ha <sup>-1</sup> )                                      |
| $EI$       | rainfall energy–intensity (N h <sup>-1</sup> )                       |
| $K$        | soil erodibility factor ((t h <sup>-1</sup> ) (ha N <sup>-1</sup> )) |
| $L_{USLE}$ | slope-length factor (–)  |
| $S_{USLE}$ | slope-steepness factor (–)   |
| $C$        | conservation factor (–)  |
| $P_{USLE}$ | support practice factor (–)  |
| $SSF$      | slope shape factor (concave, convex, uniform) (–)                    |

The slope-length and the slope–steepness factor (Wischmeier et al., 1978) are calculated by

$$L_{USLE} = \left( \frac{l}{22.14} \right)^m, \quad (11)$$

$$S_{USLE} = \frac{0.043s^2 + 0.3s + 0.43}{6.613}, \quad (12)$$

where

|     |                     |
|-----|---------------------|
| $l$ | slope length (m)    |
| $m$ | length exponent (–) |
| $s$ | slope (%)           |

Sediment discharge is calculated by the steady state continuity equation of Foster et al. (1981) and Lane (1982). Based on the Einstein (1950) approach each soil particle class (five classes are considered) is calculated separately.

$$Q_s(x) = Q_s(o) + Q_{SL} \Delta x / L_G - \int_0^x D(x) W dx, \quad (13)$$

where

- $Q_s(x)$  sediment discharge at the downstream end of the cell ( $\text{kg s}^{-1}$ )  
 $Q_s(o)$  sediment discharge at the upstream end of the cell ( $\text{kg s}^{-1}$ )  
 $Q_{SL}$  lateral sediment inflow rate ( $\text{kg s}^{-1}$ )  
 $\Delta x$  downslope distance (m)  
 $L_G$  reach length (m)  
 $D(x)$  sediment deposition rate ( $\text{kg s}^{-1} \text{m}^{-2}$ )

$$Q_s(x) = \left( \frac{2q(x)}{2q(x) + L_G V_{ss}} \right) \left[ Q_s(o) + Q_{SL} - \frac{W_m L_G}{2} \left[ \frac{V_{ss}}{q(o)} \left( q_s(o) - g_s(o) \right) - \frac{V_{ss}}{q(x)} g_s(x) \right] \right], \quad (14)$$

where

- $q(x)$  discharge per unit width exiting the cell ( $\text{m s}^{-1}$ )  
 $q(o)$  discharge per unit width entering the cell ( $\text{m s}^{-1}$ )  
 $q_s(o)$  particle discharge per unit of width into the cell ( $\text{kg s}^{-1} \text{m}^{-1}$ )  
 $W_m$  average channel width (m)  
 $V_{ss}$  particle fall velocity ( $\text{m s}^{-1}$ )  
 $g_s(o)$  effective sediment transport capacity into the cell ( $\text{kg s}^{-1} \text{m}^{-2}$ )  
 $g_s(x)$  effective sediment transport capacity out of the cell ( $\text{kg s}^{-1} \text{m}^{-2}$ )

Deposition is calculated as

$$D(x) = \frac{V_{ss}}{q(x)} [q_s(x) - g_s(x)], \quad (15)$$

where

- $D(x)$  sediment deposition rate ( $\text{kg s}^{-1} \text{m}^{-2}$ )  
 $q_s(x)$  particle discharge per unit of width ( $\text{kg s}^{-1} \text{m}^{-1}$ )

The effective sediment transport capacity is calculated using a modified Bagnold equation (Bagnold, 1966) as

$$g_s = \eta k \tau \frac{V_G^2}{V_{ss}}, \quad (16)$$

where

- $g_s$  effective sediment transport capacity ( $\text{kg s}^{-1} \text{m}^{-1}$ )  
 $\eta$  effective transport factor (–)  
 $k$  transport capacity factor (–)  
 $\tau$  shear stress ( $\text{kg m}^{-2}$ )  
 $V_G$  average channel flow velocity ( $\text{m s}^{-1}$ ).

### 3. Modifications to the AGNPS model

In an attempt to improve simulations the following modifications were integrated into the AGNPS source code:

- Replacement of the SCS curve number method by the Lutz method (1984) for calculating runoff volume.
- Replacement of the USLE *LS* factor of Wischmeier and Smith (1978) by the algorithm of Moore and Burch (1986) based on stream power theory.
- Linkage of channel erosion by individual categories of particle-size to runoff velocity.

Reasons why these modifications were thought to improve simulations are discussed below.

#### 4. Runoff calculations

Lutz (1984) published a runoff calculation method similar in concept to the CN method. He used 981 rainfall-runoff events in 75 watersheds within Germany for the development of a regionalized method for surface runoff calculation. We were interested in to test if the Lutz method outperformed the surface runoff simulations of the CN method in the two German watersheds we used in this study.

Soil data and land use were used to derive maximum discharge values (*C*-values) for each homogeneous area within a watershed. *C*-values are calculated based on a combination of soil type (hydrological soil groups A–D), land use data, AMC (II) and an extreme rainfall event of 250 mm. These values based on the watershed characteristics correspond to curve numbers. Calculation of the surface runoff by Lutz (1984) as modified by Rode (1995) is given by

$$I_a = 0.03S, \quad (17)$$

$$S = 25.4 \left( \frac{10}{C} - 10 \right), \quad (18)$$

$$a = C_1 e^{(-C_2/W_Z)} e^{(-C_3/Q_B)} e^{(-C_4 D)}, \quad (19)$$

$$Q_D = (P - I_a)C + \frac{C}{a} \left( e^{-a(P-I_a)} - 1 \right), \quad (20)$$

where

|   |   |
|---|---|
| <i>C</i>  | maximum discharge value (–)                                 |
| <i>S</i>  | potential maximum retention (mm)                            |
| <i>a</i>  | factor of proportionality ( $1 \text{ mm}^{-1}$ )           |
| <i>C</i> <sub>1</sub> , <i>C</i> <sub>2</sub> , <i>C</i> <sub>3</sub> , <i>C</i> <sub>4</sub> | weighting parameters for optimization (calibration factors) |
| <i>W</i> <sub>Z</sub>   | week value (–)  |
| <i>Q</i> <sub>B</sub>   | baseflow ( $1 \text{ sec}^{-1} \text{ km}^{-2}$ )           |
| <i>D</i>  | duration of precipitation (h)                               |

Initial abstraction (*I*<sub>a</sub>) (Eq. (17)) is calculated similar to *I*<sub>a</sub> in the CN method (Eq. (1)) but *S* (potential maximum retention) is weighted with a factor of 0.03. The Lutz method, then, uses a lower initial abstraction value, and therefore, higher surface runoff is computed (Eq. (20)), as compared to the CN method.

The week value ( $W_Z$ ) represents a simplified crop growth factor, varying during the year which affects runoff. Lutz (1984) gives a lookup table for the week value. Week values are low in summer (high crop growth), which refers to a low tendency for surface runoff generation.  $W_{ZS}$  are high in winter because of low crop growth and/or bare soils after harvest, which results in a greater tendency for surface runoff generation. The factor  $C_2$  may be used for optimization (calibration factor) to fit measured and predicted surface runoff ( $Q_D$ ). Lutz (1984) recommends fixing  $C_2$  depending on land use. The higher the values of  $C_2$ , the lower the factor of proportionality ( $a$ ), and the lower the surface runoff.

Baseflow ( $Q_B$ ) is used to characterize the initial soil moisture condition before a rainfall-runoff event takes place. Baseflow information may be derived from the interpretation of hydrographs. Lutz (1984) found that high baseflow values showed a high correlation to surface runoff, which is expressed in Eq. (19).  $C_3$  is a calibration factor weighting the influence of baseflow on surface runoff. The higher the value of  $C_3$ , the lower the factor of proportionality ( $a$ ), and the lower the surface runoff. The  $C_3$  factors in the study of Lutz (1984) ranged between 1.0 and 6.0.

The duration of precipitation characterizes the type of rainfall event, i.e., short-duration high-intensity thunderstorms or long-lasting frontal rainfall events. The shorter a precipitation event, the higher the factor of proportionality ( $a$ ), and the higher the surface runoff. The  $C_4$  is the calibration factor that weights the importance of storm duration. The higher the value of  $C_4$ , the lower the factor of proportionality ( $a$ ), and the lower the surface runoff. Lutz points out that the  $C_4$  factor may often be neglected (fixed to 0.0) because of its low sensitivity for surface runoff calculations. The  $C_1$  calibration factor is most sensitive for surface runoff. In the study of Lutz (1984), the range for  $C_1$  varied between 0.02 and 0.08.

There are contrasts between the CN and Lutz methods despite both being empirical in character. The CN method was designed for application in unmonitored watersheds without calibration. The parameterization for the Lutz method is more demanding, and calibration is recommended (Lutz, 1984). Antecedent moisture conditions (AMC) are considered in both methods; the CN approach uses hydrologic condition classification (I, II, and III), and the Lutz approach uses baseflow. The initial abstraction value is calculated differently, with the Lutz method using lower  $I_a$ s compared to the CN method.

There were differences in the calculation of initial abstraction using the CN and Lutz methods. For instance, on a homogeneous grid with forest, fair hydrologic condition, and hydrologic soil group C, the calculated  $I_a$  would be 18.8 mm (CN method) compared to 4.7 mm (Lutz method) (Table 1). A homogeneous grid with small grain, straight row, good hydrologic condition, hydrologic soil group C, would result in an  $I_a$  of 10.4 mm (CN method) compared to 1.9 mm (Lutz method). Those calculated initial abstraction values affect surface runoff calculation because no surface runoff occurs until precipitation exceeds  $I_a$ .

## 5. USLE LS factor

The sediment discharge calculation was modified by replacing the  $L$  and  $S$  factors of the USLE (Wischmeier and Smith, 1978) with algorithms based on stream power theory



Table 1  
Runoff parameters for different land use, soil, and hydrologic conditions calculated by CN and Lutz methods

| Land use                          | Treatment and hydrologic condition | Hydrologic soil group | CN method |               |                           | Lutz method         |               |                           |
|-----------------------------------|------------------------------------|-----------------------|-----------|---------------|---------------------------|---------------------|---------------|---------------------------|
|                                   |                                    |                       | CN (-)    | <i>S</i> (mm) | <i>I<sub>a</sub></i> (mm) | <i>C</i> -value (-) | <i>S</i> (mm) | <i>I<sub>a</sub></i> (mm) |
| Pasture or range forest row crops | Contoured                          | B                     | 67        | 125.1         | 25.0                      | 0.60                | 169.3         | 5.1                       |
|                                   | Poor fair                          | C                     | 73        | 93.9          | 18.8                      | 0.62                | 155.7         | 4.7                       |
|                                   | Straight row, good                 | B                     | 78        | 71.6          | 14.3                      | 0.75                | 84.7          | 2.5                       |
| Small grain                       | Straight row, good                 | C                     | 83        | 52.0          | 10.4                      | 0.80                | 63.5          | 1.9                       |
| Fallow                            | –                                  | D                     | 94        | 16.2          | 3.2                       | 0.93                | 19.1          | 0.6                       |

(Moore and Burch, 1986). The *L* and *S* factors based on stream power theory are calculated using the following equations:

$$f = \frac{A_{\text{pwa}}}{bl_{\text{pwl}}}, \quad (21)$$

$$L_{\text{sp}} = \left( \frac{fl_{\text{pwl}}}{22.14} \right)^{0.4}, \quad (22)$$

$$S_{\text{sp}} = \left( \frac{\sin s_x}{0.0896} \right)^{1.3}, \quad (23)$$

where

- f* form parameter (-)
- b* width of contour element (m)
- A<sub>pwa</sub>* partial watershed area (m<sup>2</sup>) (the upslope area draining into each pixel)
- l<sub>pwl</sub>* partial watershed length (m) (the flow length draining into each pixel)
- L<sub>sp</sub>* *L* factor (stream power theory)
- S<sub>sp</sub>* *S* factor (stream power theory)
- s<sub>x</sub>* slope (°)

These equations are more amenable to landscapes with complex topographies than the original empirical equation of Wischmeier because they explicitly account for flow convergence and divergence through the term *A<sub>pwa</sub>* in Eq. (21).

## 6. Channel erosion

Generally, discharge and flow velocity are greater for large rainfall-runoff events compared to small events, and there is a trend for increased channel scouring during large events. Factors influencing the sediment movement are the particle-size distribution, the form and weight of the particles, the cohesion between particles, the arrangement of

Table 2

Particle-size classes (mm) considered in AGNPS (Foster et al., 1980)

|                    | Primary<br>clay (clay) | Primary<br>silt (silt) | Small<br>aggregates<br>(sA) | Large<br>aggregates<br>(lA) | Primary<br>sand<br>(sand) |
|--------------------|------------------------|------------------------|-----------------------------|-----------------------------|---------------------------|
| Soils high in silt | 0.002                  | 0.01                   | 0.02                        | 0.5                         | 2.0                       |
| Soils high in clay | 0.002                  | 0.01                   | 0.075                       | 1.0                         | 2.0                       |
| Soils high in sand | 0.002                  | 0.01                   | 0.03                        | 0.2                         | 2.0                       |

particles within the channel, the geometry of the channel, the turbulence of flow, the discharge volume as well as plant and root growth (Anderson, 1988).

In AGNPS, the user has to set a flag for each grid-cell, for each particle-size class, and for each rainfall-runoff event for channel scouring. A boolean decision has to be made with flag = 1 indicating scouring of the particle class or flag = 0, no scouring of the particle class. The model considers five different particle-size classes ranging from primary clay to primary sand (Table 2).

A major drawback running the sediment routine in AGNPS is that channel scouring for each particle class is fixed subjectively by the user. To increase the objectivity within the decision process for setting flags, AGNPS was modified such that the setting of the flags (0 or 1) for channel erosion was linked to flow velocity. In Table 3, critical flow velocities are listed for each particle-size class based on the literature (Maue, 1988; DVWK, 1988). For example, if the calculated flow velocity in a grid-cell exceeds  $0.3 \text{ m s}^{-1}$  but does not exceed  $0.6 \text{ m s}^{-1}$ , then only primary clay would be scoured.

The other factors that have an impact on channel scouring were not considered because all components of the AGNPS model should be treated with a level of detail congruent with the other components of comparable importance to the simulation outcome, i.e., the new approach was selected to be of generally comparable precision with the other routines used in AGNPS.

## 7. Study areas

This study was carried out for the Glonn watersheds (Roehrs Creek —  $G_1$  and Oberdorfer Creek —  $G_2$ ) 50 km northwest of Munich (Bavaria) in Germany. The study

Table 3

Critical flow velocities ( $\text{m s}^{-1}$ ) for scouring of particle-size classes

| Flow velocity ( $\text{m s}^{-1}$ ) | Particle-size class |
|-------------------------------------|---------------------|
| 0.3                                 | Primary clay        |
| 0.6                                 | Primary silt        |
| 0.9                                 | Small aggregates    |
| 1.2                                 | Large aggregates    |
| 1.5                                 | Primary sand        |

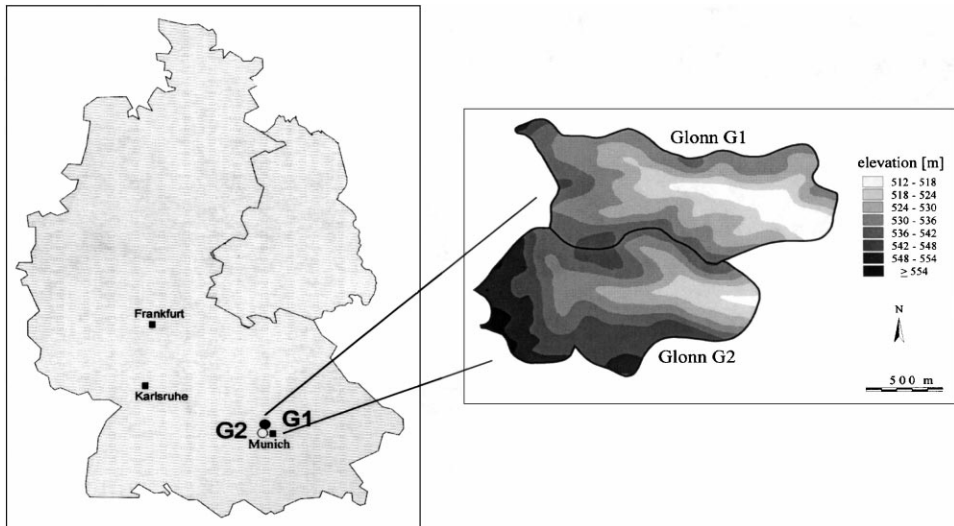


Fig. 1. Watersheds  $G_1$  and  $G_2$ .

area falls within the Tertiary Moraine Landscape of Germany. Watershed  $G_1$  is 1.2 km<sup>2</sup> and  $G_2$  is 1.6 km<sup>2</sup> in size. The elevation varies between 512–550 ( $G_1$ ) and 515–560 m ( $G_2$ ), and the average slope is 7% ( $G_1$ ) and 6% ( $G_2$ ). Fig. 1 shows the elevations for both watersheds. In watershed  $G_1$  soil texture is 44.6 % loamy sand, 7.4% clay-loam, 43.3% loam, and 4.7% sandy loam. In contrast soil texture in watershed  $G_2$  is 51.7% loamy sand, 2.8% clay-loam, and 45.5% loam. In the valley bottom, soils are more or less saturated throughout most of the year (Aqualfs). The total area covered in  $G_1$  by forest was 20.2%, while 79.8% was used as agricultural land, of which 30.9% was corn, 22.5% pasture/meadow, 32.7% grain (mainly wheat), 7.3% potatoes, 5.2% forage fodder, and 1.4% waste land. Watershed  $G_2$  was dominated by forest (58.8%), while 41.2% was used as agricultural land, of which 60.2% was grain (mainly wheat), 21.8% corn, 16.5% potatoes and 1.5% pasture/meadow. The longest pathway from the most distant point in the watershed to the drainage outlet was 1900 ( $G_1$ ) and 1800 m ( $G_2$ ), respectively. The average yearly precipitation amounts for two rain stations nearby were 830 (Mering) and 873 mm (Puch). The rainfall events used for this study varied between 17 and 89 mm, measured surface runoff ranged from 1 to 58 mm ( $G_1$ ) and 0.5 to 23 mm ( $G_2$ ), and sediment yield ranged from 0.03 to 24.5 t ( $G_1$ ) and 0.008 to 167.5 t ( $G_2$ ). For the validation of simulation results, there were 52 precipitation-runoff events available, covering a three-year period (Bavarian Water Authority, 1984).

## 8. Methods

In watershed  $G_1$ , 28 rainfall-runoff events were simulated, where 10 events were used for model calibration and 18 for validation. The total rainfall-runoff events simulated in

watershed  $G_2$  were 24, where 12 events were used for calibration and 12 for validation. A grid-size of 25 m was used.

Standard statistics and the coefficient of efficiency were calculated for measured and predicted data. When the calibration of a method was carried out, the total data set (total number of rainfall-runoff events) was divided into one subset for calibration and one for validation. A range of representative rainfall-runoff events in terms of discharge amount and seasonal occurrence were taken for calibration. Additionally, the evaluation of model outputs was based on graphical display comparing measured and predicted values for each rainfall-runoff event.

The coefficient of Nash and Sutcliffe (1970) was used as a measure of fit of actual versus predicted data. It is given by

$$E = \frac{\sum_{i=1}^n (m_i - \bar{m})^2 - \sum_{i=1}^n (p_i - m_i)^2}{\sum_{i=1}^n (m_i - \bar{m})^2}, \quad i = 1, 2, \dots, n, \quad (24)$$

where

$m_i$  measured variable

$p_i$  predicted variable

$\bar{m}$  arithmetic mean of  $m_i$  for all events  $i = 1$  to  $n$ .

The calculation of  $E$  is a procedure which essentially is the sum of the deviations of the observations from a linear regression line with a slope of 1. If the measured variable is predicted exactly for all observations the model  $E$  is 1. Low values of  $E$  represent high deviations between measured and predicted values. If  $E$  is negative predictions are very poor and an average value for output is a better estimate than the model prediction.

The modeling framework was comprised of the geographic information system (GIS) SPANS, an input interface, the AGNPS model, and an output interface. The modifications of algorithms were integrated in the source code of AGNPS. Further details about the automated modeling framework and the input data are given in Grunwald (1997).

## 9. Results and discussion

### 9.1. Surface runoff

To compare different surface runoff calculations, three different variants were considered:

1. Uncalibrated CN method. Variant:  $Q_1$ .
2. Calibrated CN method. Variant:  $Q_2$ .
3. Calibrated Lutz method. Variant:  $Q_3$ .

### 9.2. Variant $Q_1$

Surface runoff was calculated using the existing AGNPS model, i.e., using the CN method without calibration for runoff volume. In Fig. 2, the variations between measured and predicted surface runoff calculated by SCS CN method for both watersheds are

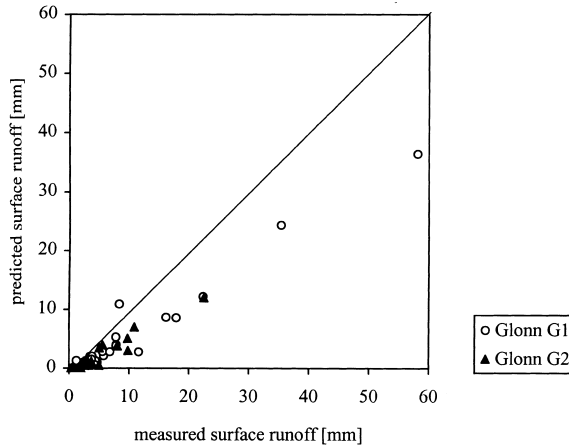


Fig. 2. Measured and predicted surface runoff calculated by uncalibrated CN method (variant  $Q_1$ ).

shown. For most of the events (<50 mm precipitation amount), almost no runoff was calculated. The graph shows that almost all rainfall events were underestimated by the uncalibrated CN method compared to the measured surface runoffs. Deviations between measured and predicted surface runoff were greater for smaller events (<10 mm  $Q_D$ ) than for larger events (>10 mm  $Q_D$ ).

Statistics comparing measured and predicted surface runoff for the validation rainfall-runoff events are shown in Table 4. Coefficients of efficiency ( $E$ ) of 0.25 (watershed Glonn  $G_1$ ) and 0.24 (watershed  $G_2$ ) were calculated and shown to be very low compared to an ideal  $E$  of 1. In watershed  $G_1$ , the median for 28 measured events was 4.5 mm, which was higher than the median for the predicted events (2.0). In watershed Glonn  $G_2$ ,

Table 4

Surface runoff (in mm) for validation of CN and Lutz method using AGNPS and modified versions in  $G_1$  and  $G_2$  watersheds

| $n$           | Watershed Glonn $G_1$   |                         |            |                  |      | Watershed Glonn $G_2$ |            |            |                  |      |
|---------------|-------------------------|-------------------------|------------|------------------|------|-----------------------|------------|------------|------------------|------|
|               | 28                      |                         | 18         |                  |      | 24                    |            | 12         |                  |      |
|               | M <sup>a</sup><br>$Q_D$ | P <sup>b</sup><br>$Q_1$ | M<br>$Q_D$ | P<br>$Q_2$ $Q_3$ |      | M<br>$Q_D$            | P<br>$Q_1$ | M<br>$Q_D$ | P<br>$Q_2$ $Q_3$ |      |
| Mean [mm]     | 9.0                     | 4.9                     | 9.0        | 8.6              | 8.7  | 4.4                   | 1.8        | 3.2        | 4.1              | 4.3  |
| S. E. [mm]    | 2.3                     | 1.5                     | 3.2        | 2.5              | 2.7  | 1.0                   | 0.6        | 1.1        | 0.8              | 0.8  |
| Median [mm]   | 4.5                     | 2.0                     | 3.8        | 5.2              | 4.3  | 3.0                   | 0.6        | 2.0        | 2.9              | 2.7  |
| Minimum [mm]  | 0.7                     | 0.04                    | 0.7        | 1.1              | 1.0  | 0.3                   | 0          | 0.5        | 2.0              | 1.4  |
| Maximum [mm]  | 58.1                    | 36.4                    | 58.1       | 46.2             | 50.0 | 22.5                  | 12.0       | 10.9       | 10.4             | 9.7  |
| Standard [mm] | 12.3                    | 8.1                     | 13.4       | 10.7             | 11.6 | 4.9                   | 2.9        | 3.6        | 2.9              | 3.1  |
| $E$ [-]       | –                       | 0.25                    | –          | 0.93             | 0.96 | –                     | 0.24       | –          | 0.76             | 0.83 |

<sup>a</sup> Measured.

<sup>b</sup> Predicted.

the median for 24 measured events was 3.0 mm, which differs from the predicted median for surface runoff of 0.6 mm.

### 9.3. Variant $Q_2$

Because surface runoff using the uncalibrated curve number method was not predicted well, a calibration was carried out. From the total number of events, a range of representative rainfall-runoff events in terms of discharge amount and seasonal occurrence were taken for calibration (10 and 12 calibration events in watershed  $G_1$  and  $G_2$ , respectively). The objective of the calibration procedure was to optimize  $x$  in the equation  $I_a = x \times S$  (Eq. (1)) in such a manner that the calculated coefficient of efficiency ( $E$ ) for all calibration events would be highest. During the calibration procedure, all input parameters were kept constant except  $x$ , which was varied between 0.01 and 0.4. Afterwards, the optimized equation was used for validation. In watershed  $G_1$  the highest  $E$  was found when  $x$  was 0.03 ( $E$ : 0.87), and in watershed  $G_2$  the highest  $E$  was found when  $x$  had a value of 0.05 ( $E$ : 0.86).

The validation results using the calibrated curve number method are shown in Figs. 3 and 4. The points are scattered closer to the line of equal values compared to variant  $Q_1$ . Table 4 shows a median for 18 measured validation rainfall-runoff events in  $G_1$  watershed of 3.8 mm and a median of 5.2 mm for predicted surface runoff. The measured median for 12 validation rainfall-runoff events in  $G_2$  of 2.0 mm was lower compared to the predicted median of 2.9 mm. The coefficient of efficiency for all validation events was 0.93 for  $G_1$  and 0.76 for  $G_2$ .

### 9.4. Variant $Q_3$

For comparison, the Lutz method was used to calculate surface runoff in the Glonn watersheds. The calibration events chosen for variants  $Q_1$  and  $Q_2$  were also used for

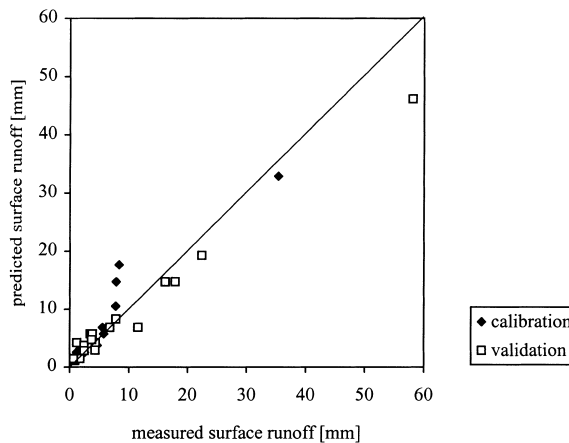


Fig. 3. Measured and predicted surface runoff calculated by calibrated CN method (variant  $Q_2$ ) —  $G_1$  watershed.

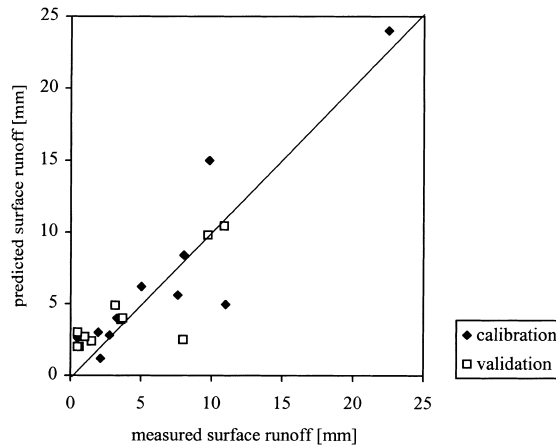


Fig. 4. Measured and predicted surface runoff calculated by calibrated CN method (variant  $Q_2$ ) —  $G_2$  watershed.

analysis in variant  $Q_3$ . The  $C_2$  factor was determined depending on land use as proposed by Lutz (forest 2.0; permanent pasture 2.0; grain 3.0; corn 4.6; potatoes (other row crops) 4.6; wasteland 4.0). The objective of the calibration procedure was to optimize the parameters  $C_1$  and  $C_3$  in such a manner that the coefficient of efficiency would be highest for the calibration events considered. During the calibration procedure, all input parameters were kept constant except  $C_1$  and  $C_3$ . According to the calibration procedure, a  $C_1$  value of 0.06 and  $C_3$  of 4.0 provided the best fit for watershed  $G_1$ . In watershed  $G_2$  the same calibration method was used, and a  $C_1$  value of 0.04 and  $C_3$  of 4.0 demonstrated the best fit.

The validation results are shown in Figs. 5 and 6. Measured and predicted surface runoff values are very near the 1:1 line. Results in Table 4 indicate that the deviations between measured and predicted medians were 0.5 ( $G_1$ ) and 0.7 mm ( $G_2$ ), which were lower compared to the results from the CN method (variants  $Q_1$  and  $Q_2$ ). The  $E$  for the validation rainfall-runoff events was 0.96 ( $G_1$ ) and 0.83 ( $G_2$ ), which outperformed the predictions by both the uncalibrated and the calibrated CN method.

## 10. Sediment yield and channel erosion

Three different sediment yield calculations were considered:

1. Modified USLE (Eqs. (10)–(12)). Output: sediment yield  $S_1$ .
2.  $LS$  algorithm by Moore and Burch (1986) (Eqs. (21)–(23)). Output: sediment yield  $S_2$ .
3.  $LS$  algorithm by Moore and Burch (1986) plus linkage of channel erosion by individual particle-size categories to flow velocity. Output: sediment yield  $S_3$ .

For all sediment yield calculations, surface runoff was calculated based on the Lutz method because this method gave the best outputs in both watersheds. Therefore, the

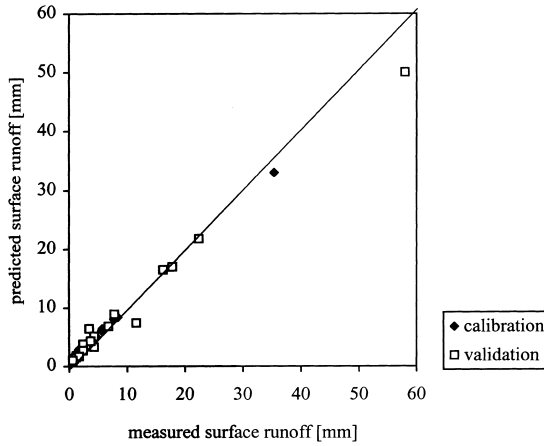


Fig. 5. Measured and predicted surface runoff calculated by calibrated Lutz method (variant  $Q_3$ ) —  $G_1$  watershed.

different outputs of the variants  $S_1$ ,  $S_2$ , and  $S_3$  can be analyzed without bias from the hydrology component. The same errors due to hydrology predictions in AGNPS act on variants  $S_1$ ,  $S_2$ , and  $S_3$  for sediment transport calculations.

### 10.1. Variant $S_1$

Flags for the scouring of particle-sizes for each grid-cell had to be set for the sediment yield calculations. A calibration was carried out to optimize the decision for channel scouring. From the total samples, representative rainfall-runoff events were taken for

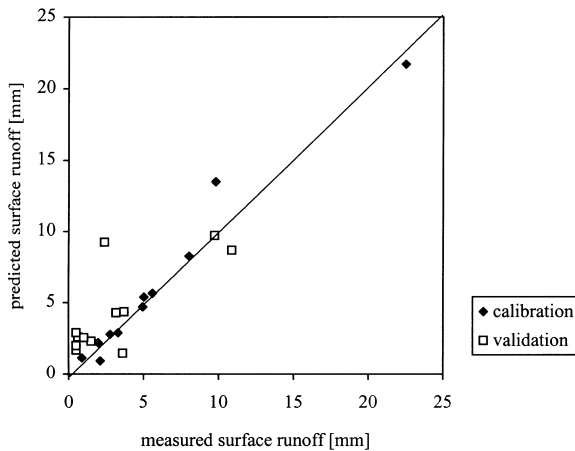


Fig. 6. Measured and predicted surface runoff calculated by calibrated Lutz method (variant  $Q_3$ ) —  $G_2$  watershed.



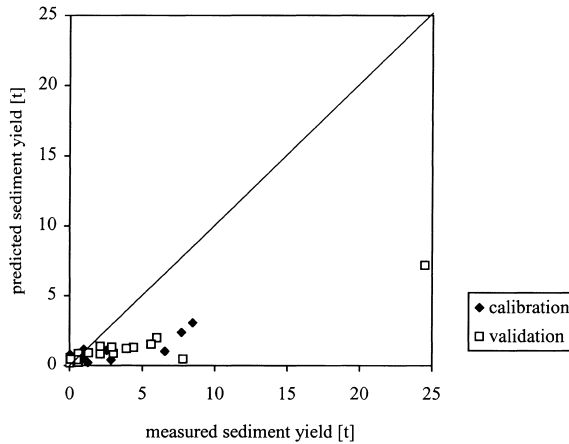


Fig. 7. Measured and predicted sediment yield  $S_1$  —  $G_1$  watershed.

calibration (10 and 12 calibration events in watershed  $G_1$  and  $G_2$ , respectively). The objective was to identify a combination of flags for particle-size classes that optimize the coefficient of efficiency. The highest  $E$  (0.42) was calculated for the combination specifying ‘no scouring of particles’. In Fig. 7 the measured and predicted sediment yields ( $S_1$ ) in  $G_1$  watershed are shown. The sediment yield for many rainfall-runoff events was considerably underpredicted compared to measured values. The measured and predicted sediment yields ( $S_1$ ) calculated for  $G_2$  watershed are shown in Fig. 8. The points are scattered, which indicates poor predictions. Statistics in Table 5 confirm the tendency of underpredictions in sediment yield ( $S_1$ ) when compared to measured values. For example, the median for 18 measured validation events was 2.1 t compared to the median for predicted events of 0.9 t in  $G_1$  watershed. In watershed  $G_2$  the median for measured

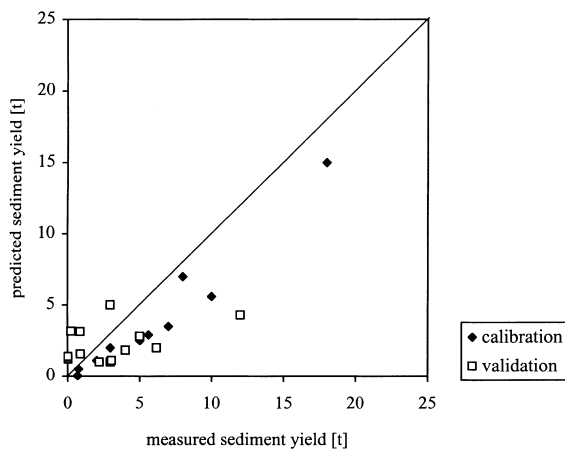


Fig. 8. Measured and predicted sediment yield  $S_1$  —  $G_2$  watershed.

Table 5

Sediment yield results for validation of variants  $S_1$ ,  $S_2$  and  $S_3$  in the  $G_1$  and  $G_2$  watersheds

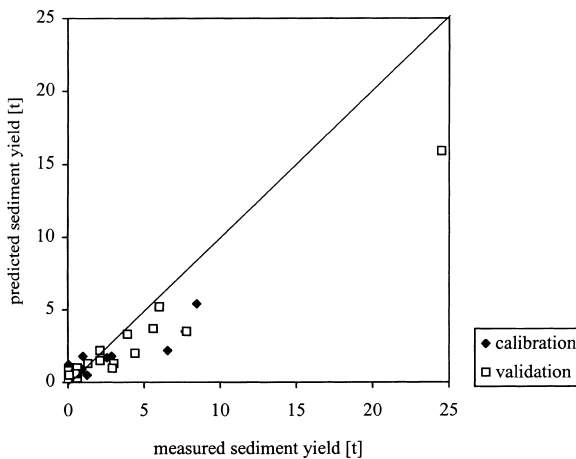
| <i>n</i>     | Watershed Glonn G1 |                |       |      |       | Watershed Glonn G2 |       |       |      |       |
|--------------|--------------------|----------------|-------|------|-------|--------------------|-------|-------|------|-------|
|              | 28                 |                | 18    |      |       | 24                 |       | 12    |      |       |
|              | M <sup>a</sup>     | P <sup>b</sup> |       | M    | P     | M                  | P     |       | M    | P     |
|              |                    | $S_1$          | $S_2$ |      | $S_3$ |                    | $S_1$ | $S_2$ |      | $S_3$ |
| Mean [t]     | 3.6                | 1.2            | 1.9   | 3.5  | 3.0   | 2.9                | 2.1   | 2.2   | 4.2  | 4.2   |
| S. E. [t]    | 1.4                | 0.4            | 0.9   | 0.9  | 0.8   | 0.9                | 0.3   | 0.4   | 0.9  | 0.8   |
| Median [t]   | 2.1                | 0.9            | 1.1   | 2.1  | 2.0   | 2.6                | 1.2   | 1.6   | 3.0  | 3.1   |
| Minimum [t]  | 0                  | 0.18           | 0.25  | 0    | 0.05  | 0.01               | 0.8   | 0.8   | 0.01 | 0.75  |
| Maximum [t]  | 24.5               | 7.2            | 15.9  | 24.5 | 21.0  | 12.0               | 5.0   | 5.5   | 18.0 | 17.0  |
| Standard [t] | 5.7                | 1.6            | 2.7   | 4.9  | 4.1   | 3.2                | 1.2   | 1.3   | 4.4  | 3.4   |
| <i>E</i> [-] | –                  | 0.26           | 0.57  | –    | 0.90  | –                  | 0.57  | 0.60  | –    | 0.72  |

<sup>a</sup> Measured.<sup>b</sup> Predicted.

validation events was 2.6 t compared to the median for predicted events of 1.2 t. The coefficient of efficiency was 0.26 in  $G_1$  watershed and 0.57 in  $G_2$  watershed, which is poor compared with the ideal *E* of 1.

### 10.2. Variant $S_2$

The same calibration procedure was carried out for variant Q2, where soil loss was calculated based on the algorithm of Moore and Burch (1986). The highest *E* (0.65) was calculated for the combination specifying ‘no scouring of particles’. In Figs. 9 and 10 the measured and predicted sediment yields ( $S_2$ ) are presented. There is an underprediction in sediment yield when compared to the measured values. In watershed  $G_1$  there is an

Fig. 9. Measured and predicted sediment yield  $S_2$  —  $G_1$  watershed.

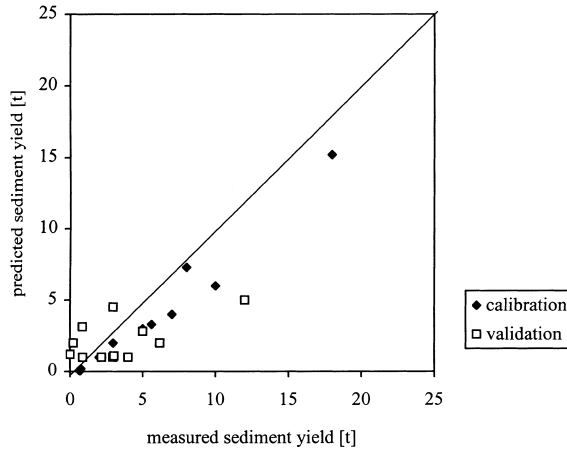


Fig. 10. Measured and predicted sediment yield  $S_2$  —  $G_2$  watershed.

improvement in sediment yield predictions when compared to  $S_1$ , while the improvement in sediment yield predictions in watershed  $G_2$  was limited. Table 5 indicates that the deviations between measured and predicted medians were 1.0 t (watershed  $G_1$  and  $G_2$ ), which was lower compared to variant  $S_1$ . The  $E$  was 0.57 ( $G_1$ ) and 0.60 ( $G_2$ ), which was an improvement in the sediment yield calculations compared to  $S_1$ , but were still low when compared to an ideal  $E$  of 1.

### 10.3. Variant $S_3$

No calibration was necessary for variant Q3 because setting of flags for channel scouring was linked to flow velocity. In Fig. 11, measured versus predicted sediment

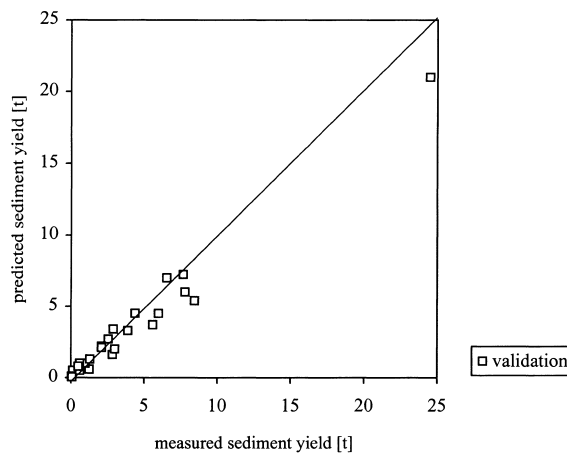


Fig. 11. Measured and predicted sediment yield  $S_3$  —  $G_1$  watershed.

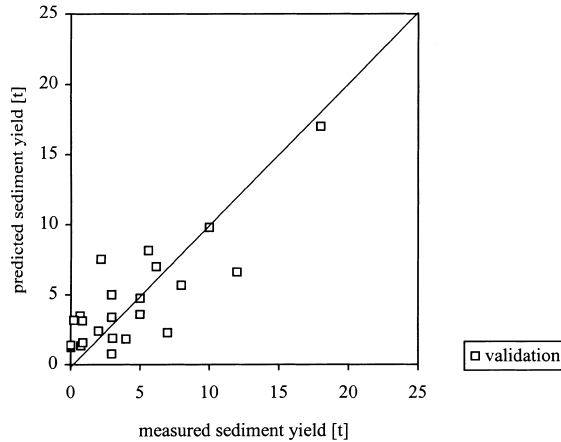


Fig. 12. Measured and predicted sediment yield  $S_3$  —  $G_2$  watershed.

yield calculations are shown for the  $G_1$  watershed, which are scattered rather equally around the 1:1 line. Fig. 12 shows measured versus predicted sediment yield for the  $G_2$  watershed, where the points are more scattered around the 1:1 line. In Table 5, the results for  $S_3$  predictions indicated an improvement when compared to  $S_2$  and  $S_1$  predictions. In watershed  $G_1$ , the measured median for 18 validation events yielded 2.1 t which is close to the predicted median of 2.0 t. The deviation between measured and predicted median was 0.1 t which outperformed variants  $S_1$  and  $S_2$ . In watershed  $G_2$ , the median for 12 validation events was 3.0 (measured) and 3.1 t (predicted). The coefficient of efficiency was 0.90 (Glenn  $G_1$ ) and 0.72 (Glenn  $G_2$ ) which was considerably better than variant  $S_1$  and  $S_2$  because the  $E_s$  were closer to 1.

## 11. Conclusions

Simulations of surface runoff and erosion with AGNPS and modified versions were used to (i) investigate model performance, and (ii) to describe the drainage behavior and sediment loss at the drainage outlet of two small agricultural watersheds. The long-term goal in management of these agricultural waters is to maximize soil and water quality.

A comparison between three different surface runoff methods,  $Q_1$ ,  $Q_2$ , and  $Q_3$  showed that calibration improved the agreement between measured and predicted surface runoff values to a high degree. The replacement of CN with Lutz method improved the predictions only slightly beyond that. For the uncalibrated CN method poor results were predicted compared to measured surface runoff values. Results showed that calibration of CN method and Lutz method improved surface runoff predictions. A calibration of model predictions is often not possible because of a lack in measured data, however, as shown in this study, there is merit in calibrating a simulation model such as AGNPS. The improvements in predictions of Lutz method when compared to calibrated CN method are merely the result of having additional parameters to fit the data ( $C_1$ ,  $C_2$ ,  $C_3$ ,  $C_4$

calibration parameters). Land use pattern and soils influence the infiltration and surface runoff behavior. Generally, high surface runoff predictions were calculated for (i) silt-rich soils in the valley bottoms, (ii) high CN values (CN method) or high  $C$  values (Lutz method), and/or (iii) locations with high values in upslope drainage area.

In AGNPS sediment yield calculations depend on (i) soils (soil erodibility factor — USLE), (ii) topography (slope-length factor, slope-steepness factor, slope shape factor — USLE), (iii) land use and management (conservation factor and support practice factor — USLE), (iv) discharge and sediment yield flowing into the grid-cell, (v) erosion and deposition within the grid-cell, and (vi) sediment transport capacity, which determines the sediment rate flowing out of the grid-cell.

The comparison between three variants in the sediment yield calculation demonstrated an improvement of model outputs using the proposed modifications in sediment yield calculation. Using variant  $S_3$ , no calibration in sediment yield calculations was necessary because flags for channel scouring of particles were set automatically. This fact will prove beneficial to users.

In variant  $S_1$  sediment yield predictions matched best measured values using the assumption ‘no scouring’ for channel erosion in both watersheds. This contradicts with observations in the field, where channel erosion was observed for large rainfall-runoff events. Variant  $S_3$  outperformed variant  $S_1$  and  $S_2$  in sediment yield predictions. The key for this result is seen in the description of scouring of particles in channels, where flow velocity is used for decision making about scouring of each particle class in each grid-cell individually. The method for channel scouring in  $S_3$  is more objective than the method used in  $S_1$  and thus more beneficial for AGNPS users.

Variant  $S_2$  improved sediment yield predictions when compared to  $S_1$ . The improved sediment yield predictions can be traced back to the consideration of the upslope drainage area ( $A_{pwa}$ ) and their characteristics (slope and shape) in the soil loss calculation (Eqs. (10), (21)–(23)).

Validation results of this study illustrated that a calibration of CN method (or Lutz method) for surface runoff calculations and the use of variant  $S_3$  for sediment yield calculations with AGNPS model showed the highest merit to match measurements with predictions at the drainage outlet.

## Acknowledgements

The project was sponsored by a fellowship of the State Hessen, Germany.

## References

- Anderson, M.G., 1988. *Modelling Geomorphological Systems*. Wiley, Chichester, UK.
- Bagnold, R.A., 1966. *An approach to the sediment transport problem from general physics*. US Geological Survey Professional Paper 422-I, Washington, DC, USA.
- Bavarian Water Authority, 1984. *Naehrstoffaustrag aus landwirtschaftlich genutzten Flaechen*.
- DVWK, 1988. *DVWK-Schriften. Feststofftransport in Fliessgewaessern — Berechnungsverfahren fuer die Ingenieurspraxis*, vol. 87. Paul Parey, Hamburg, Berlin.

- Einstein, H.A., 1950. The bed-load function for sediment transportation in open channel flows. Technical Bulletin No. 1026. US Department of Agriculture, Soil Conservation Service, Washington, DC, USA.
- Engel, B.A., Srinivasan, R., Arnold, J., Rewerts, C., Brown, S.J., 1993. Non-point source (NPS) pollution modeling using models integrated with geographic information systems (GIS). *Water Sci. Technol.* 28 (3-5), 685–690.
- Feezor, D.R., Hirschi, M.C., Lesikar, B.J., 1989. Effect of cell size on AGNPS prediction. In: ASAE Winter Meeting in New Orleans, 12–15 December 1989. ASAE Paper No. 89-2662.
- Fisher, P., Abrahart, R.J., Herbinger, W., 1997. The sensitivity of two distributed non-points source pollution models to the spatial arrangement of the landscape. *Hydrol. Process.* 11, 241–252.
- Foster, G.R., Lane, L.J., Nowlin, J.D., 1980. A model to estimate sediment yield from field-sized areas: selection of parameter values. In: Knisel, W.G. (Ed.), CREAMS: A field-scale model for chemicals, runoff, and erosion from agricultural management systems. Conservation Research Report No. 26, US Department of Agriculture.
- Foster, G.R., Lane, L.J., Nowlin, J.D., Laffen, L.M., Young, R.A., 1981. Estimating erosion and sediment yield on field-sized areas. *Trans. ASAE* 24 (5), 1253–1262.
- Grunwald, S., 1997. GIS-gestuetzte Modellierung des Landschaftswasser und Stoffhaushaltes mit dem Modell AGNPSm, vol. 14. Ph.D. Dissertation, Department of Natural Resources Management, Giessen University, Boden und Landschaft.
- Grunwald, S., Haverkamp, S., Bach, M., Frede, H.-G., 1997. Ueberpruefung von MEKA-massnahmen zum erosions und gewaesserschutz durch das modell AGNPSm (Assessment of MEKA subsidies for soil and water protection by AGNPSm). *J. Rural Eng. Development* 38 (6), 260–265.
- Hession, W.C., Huber, K.L., Mostaghimi, S., Shanholtz, V.O., McClellan, P.W., 1989. BMP effectiveness evaluation using AGNPS and a GIS. In: International Winter Meeting in New Orleans, Louisiana, 12–15 December 1989. Paper No. 89-2566. *Am. Soc. Agric. Eng.*, pp. 1–18.
- Lane, L.J., 1982. Development of a procedure to estimate runoff and sediment transport in ephemeral streams. In: Recent Developments in the Explanation and Prediction of Erosion and Sediment Yield, Publication No. 137. International Association of Hydrological Science, Wallingford, England, pp. 275–282.
- Lutz, W., 1984. Berechnung von Hochwasserabflüssen unter Anwendung von Gebietskenngrößen. Ph.D. Thesis. Karlsruhe University, p. 235.
- Maue, G., 1988. DVWK-Schriften. Literaturstudie zur Freisetzung von Nachstoffen aus Sedimenten in Fließgewässern. Paul Parey, Hamburg, Berlin, pp. 273–344.
- Mitchell, J.K., Engel, B.A., Srinivasan, R., Wang, S.S.Y., 1993. Validation of AGNPS for small watersheds using an integrated AGNPS/GIS system. *Water Resources Bull.* 29 (5), 833–842.
- Moore, I.D., Burch, G.J., 1986. Physical basis of the length-slope factor in the Universal Soil Loss Equation. *Soil Sci. Soc. Am. J.* 50, 1294–1298.
- Nash, J.E., Sutcliffe, J.V., 1970. River flow forecasting through conceptual models. I. A discussion of principles. *J. Hydrol.* 10, 282–290.
- Needhan, S., Vieux, B., 1989. A GIS for AGNPS parameter input and mapping output. In: International Winter Meeting by the American Society of Agricultural Engineers, New Orleans, Louisiana, 1989, Paper No. 89-2673.
- Olivieri, L.J., Schaal, G.M., Logan, T.J., Elliot, W.J., Motch, B., 1991. Generating AGNPS input parameter using remote sensing and GIS. In: International Winter Meeting by the ASAE, Hyatt Regency, Chicago, IL, 1991, Paper No. 91-2622.
- Panuska, J.C., Moore, I.D., Kramer, L.A., 1991. Terrain analysis: integration into the Agricultural Non-point Source (AGNPS) Pollution Model. *J. Soil Water Conserv.*, Jan.–Feb., pp. 59–64.
- Prato, T., Shi, H., 1990. A comparison of erosion and water pollution control strategies for an agricultural watershed. *Water Resources Res.* 26 (2), 199–205.
- Rode, M., 1995. Quantifizierung der Phosphorbelastung von Fließgewässern durch landwirtschaftliche Flächennutzung, vol. 1. Ph.D. Dissertation. Department of Natural Resources Management, Giessen University, pp. 168.
- Rode, M., Grunwald, S., Frede, H.-G., 1995. Methodik zur GIS-gestuetzten Berechnung von Nachstoffeinträgen in Fließgewässern durch Oberflächenabfluß mit dem Modell AGNPS. *J. Rural Eng. Dev.* 36, 63–68.

- Smith, R.E., Williams, J.R., 1980. Simulation of the surface water hydrology. In: Knisel W.G. (Ed.), *CREAMS: A Field-Scale Model for Chemicals, Runoff and Erosion from Agricultural Management Systems*, vol. 26. USDA, Conservation Research Report, pp. 13–35.
- SCS-USDA, 1972. *National Engineering Handbook, Section 4. Hydrology*.
- SCS-USDA, 1985. *National Engineering Handbook, Section 4. Hydrology*. US Government Printing Office, Washington, DC, USA.
- Srinivasan, R., Engel, B.A., 1994. A spatial decision support system for assessing agricultural non-point source pollution. *Water Resources Bull.* 30 (3), 441–452.
- Tim, U.S., Jolly, R., 1994. Evaluating agricultural non-point source pollution using integrated geographic information system and hydrologic/water quality model. *J. Environ. Qual.* 23, 25–35.
- Tim, U.S., Mostaghimi, S., Shanholtz, V.O., 1992. Identification of critical non-point pollution source areas using geographic information systems and water quality modeling. *Water Resources Bull.* 28 (8), 877–887.
- Vieux, B.E., Needhan, S., 1993. Non-point pollution model sensitivity to grid-cell size. *J. Water Resources Planning Mgmt.* 119, 141–157.
- Wischmeier, W., Smith, D., 1978. *Predicting Rainfall Erosion Losses — A Guide to Conservation Planning*. USDA Handbook No. 537.
- Young, R.A., Onstad, C.A., Bosch, D.D., Anderson, W.P., 1987. *AGNPS, Agricultural Non-Point Source Pollution Model — A Watershed Analysis Tool*, vol. 35. USDA Conservation Research Report, pp. 1–80.
- Young, R.A., Onstad, C.A., Bosch, D.D., Anderson, W.P., 1989. *AGNPS: a non-point source pollution model for evaluating agricultural watersheds*. *J. Soil Water Conserv.* 44 (2), 168–173.
- Young, R.A., Onstad, C.A., Bosch, D.D., Anderson, W.P., 1994. *Agricultural Non-Point Source Pollution Model. AGNPS User's Guide*.